Adsorption of Lysozyme over Mesoporous Molecular Sieves MCM-41 and SBA-15: Influence of pH and Aluminum Incorporation

A. Vinu,[†,‡] V. Murugesan,[‡] and Martin Hartmann*[,†]

Department of Chemistry, Chemical Technology, Kaiserslautern University of Technology, P.O. Box 3049, D-67653, Kaiserslautern, Germany, and Department of Chemistry, Anna University, Chennai-600025, India

Received: October 31, 2003; In Final Form: January 20, 2004

The adsorption of lysozyme on the mesoporous molecular sieves MCM-41 and SBA-15 from buffered solutions with different pH values has been studied as a model protein adsorption system. The amount adsorbed depends on the solution pH as well as on the pore volume and the composition of the adsorbent. The adsorption isotherms at pH 6.5 to 10.5 fitted the Langmuir model (type L isotherm), while the isotherms recorded at pH 12 are of the S type. The maximum amount adsorbed was observed for AlSBA-15 at pH 9.6 and amounted to 47.2 μmol/g (580 mg/g). The stability of SBA-15 toward to the buffer solution is higher for SBA-15 as compared to MCM-41, which is probably a consequence of the higher wall thickness of the former material. Diffuse reflectance Fourier transform infrared spectra of the adsorbed lysozyme confirm that the adsorption of the enzyme did not result in denaturation of Lz.

Introduction

The adsorption of proteins from solution onto solid surfaces has attracted much attention due to its scientific importance and application in many areas.[1−3] For example, in the medical and food industries, it is essential to remove adsorbed proteins since even a small amount of deposited proteins may give rise to the subsequent adsorption of fibrous proteins leading to adverse biological consequences.[4−6] Protein adsorption can also contribute to blood clotting and heart disease.[7] The adsorption of proteins on inorganic materials is crucial because of the potential to improve the stability of enzymes under extreme conditions.[8] The controlled adsorption of proteins is essential in the field of enzymatic catalysis, biosensors, and disease diagnostics.[9−11]

Adsorption of protein over sol−gels and controlled porous glass (CPG) has been extensively studied for possible applications as biosensors[12−15] and reviewed by Weetall[12] and Avnir.[13] However, sol−gels are found to be unsuitable for the immobilization of proteins due to their broad pore size distribution.[14] On the other hand, the major disadvantage of CPG materials for adsorption studies are their high cost and more importantly their surface area, which rapidly decreases with increasing pore size (30−200 nm).[15] The discovery of mesoporous silicate molecular sieves opened up new possibilities in many areas of chemistry and material science.[16−18] These materials possess high specific surface areas, high specific pore volumes, and well-ordered pore structures with uniform mesopores adjustable from about 1.5 to 10 nm. Mesoporous materials have a clear advantage over microporous zeolites and zeotype molecular sieves for the adsorption and transformation of large organic molecules.[19−21]

The adsorption and separation of proteins and other biologically relevant molecules such as amino acids with nanoporous materials have been recently reviewed by Daehler et al.[22] Moreover, on mesoporous supports immobilized enzymes have been tested as enzymatic catalysts on mesoporous supports.[23−26] In the majority of those studies, the catalytic activity of the enzyme was assessed by using the typical assay for each enzyme. Takahashi et al.[27] reported the catalytic activity of horseradish peroxidase immobilized on mesoporous supports in the oxidation of 1,2-diaminobenzene. Gomez et al.[28] studied the transesterification of *N*-acetyl-L-tyrosine ethyl ester with propan-1-ol using trypsin supported on MCM-41 as a catalyst.

The protein hen egg white lysozyme (Lz) has received particular attention because of its well-understood structural characteristics.[29] Lz is an antimicrobial protein that is prevalent in ocular fluid, thus the adsorption of Lz on contact lenses is a considerable problem in ophthalmology.[30] It is a small globular protein (molecular mass 14 400 Da) with 18 cationic amino acid residues (6 lysyl including 1 N-terminal, 11 arginyl, and 1 histidyl) and 12 anionic residues (2 glutamyl, 9 aspartyl, and 1 leucyl C-terminal).[31] Lysozyme has a single peptide chain of a total of 129 amino acids in which 4 pairs of cysteins form disulfide bridges between positions 6 and 127, 30 and 115, 64 and 80, and 76 and 94. Lz has a prolate spheroid shape with two characteristic cross sections: a side of dimensions of roughly 3.0 × 4.5 nm^2 and an end of dimensions 3.0 × 3.0 nm^2.[32] The isoelectric point of Lz is around 11.[33] The isoelectric point is the pH value in solution at which the sum of the charges on the protein is zero. From the X-ray crystal structure study it can be seen that Lz is a hard protein up to ionic strengths of at least 0.4 and has both hydrophobic and hydrophilic amino acids exposed to the exterior.[33,34] It also has been reported that Lz is a rigid and stable enzyme because the four internal disulfide bonds help maintain its tertiary structure.[29] In the range of physiological temperature, no detectable change in the structure was observed within the pH range from 1.5 to 12. The adsorption of Lz onto silica and silica−titania at neutral pH has been studied previously, using different methods such as in situ ellipsometry,[35] neutron reflection,[36] fluorescence with total internal reflection,[37] UV absorbance,[38] and time-resolved optical waveguide lightmode spectroscopy (OWLS).[39−41] Al-

* Author to whom correspondence should be addressed. Phone: +49-631-205-3559. Fax: +49-631-205-4193. E-mail: hartmann@rhrk.uni-kl.de.
† Kaiserslautern University of Technology.
‡ Anna University.

10.1021/jp037303a CCC: $27.50
Published on Web 05/01/2004

though the adsorption of various proteins over mesoporous materials has been studied by several authors, little attention has been given to lysozyme. Kisler et al.[42,43] reported the adsorption of Lz on MCM-41 and surface-coated MCM-41. They found that the coated material shows a higher adsorption capacity as compared to the parent material MCM-41. However, the influence of the solution pH, the pore size of the mesoporous adsorbent, and the difference in adsorption behavior of pure silica and aluminum-substituted mesoporous materials have not been studied up till now.

The present work describes the adsorption of Lz over MCM-41, AlMCM-41, SBA-15, and AlSBA-15 materials with different pore diameters. The influence of the solution pH on the amount of Lz adsorbed over different adsorbents is also reported. It has been found that the amount of Lz adsorption on the aluminum-substituted mesoporous adsorbents is higher as compared to their pure silica analogues. Moreover, the amount of Lz adsorption is maximal near the isoelectric point. In addition, all adsorbents have been characterized by XRD, N_2 adsorption, and FT-IR spectroscopy after adsorption and desorption to ensure the structural stability of the adsorbent and the adsorbate.

Experimental Section

Materials. Hen egg white lysozyme (3× crystallized, lyophilized, activity 25.000 units/mg of protein) was obtained from ICN biomedicals (Catalog No. 100831) and used without further purification. Pure silica MCM-41 and aluminum-substituted AlMCM-41 materials with different pore diameters were synthesized with use of dodecyltrimethylammonium bromide (C_{12}-(Al)MCM-41) and hexadecyltrimethylammonium bromide (C_{16}-(Al)MCM-41), respectively, as reported earlier.[44,45] SBA-15 and AlSBA-15 were synthesized by using the tri-block copolymer poly(ethylene glycol)-*block*-poly(propylene glycol)-*block*-poly(ethylene glycol) (Pluronic P123, molecular weight 5800, $EO_{20}PO_{70}EO_{20}$) as described in our previous paper.[45]

Characterization. The X-ray powder diffraction patterns were recorded on a Siemens D5005 diffractometer with use of Cu Kα radiation. Nitrogen adsorption and desorption isotherms were measured at 77 K on a Quantachrome Autosorb 1 sorption analyzer. All samples were outgassed at 513 K for 3 h prior to the adsorption measurements. The specific surface area was obtained by using the standard Brunauer−Emmett−Teller (BET) method, while the pore size distribution was calculated from the adsorption branch of the isotherm by using the Nonlocal Density Functional Theory (NLDFT). Diffuse reflectance Fourier transform infrared (DRIFT) spectra were recorded on a Nicolet Nexus instrument equipped with a SpectraTech diffuse reflectance cell. The spectra were obtained by averaging 200 scans with a resolution of 8 cm^{-1}.

Lysozyme Adsorption. A series of standard Lz solutions with concentrations ranging from 17 to 280 μmol/L was prepared by dissolving different amounts of Lz in 25 mM buffer solutions (pH 6.5 potassium phosphate buffer, pH 9.6, 10.5, and 12 sodium bicarbonate buffer). In each adsorption experiment, 20 mg of the different mesoporous adsorbents was suspended in 4 g of the respective Lz solution. The resulting mixture was continuously shaken in a shaking bath with a speed of 160 shakes/min at 293 K until equilibrium was reached (typically 96 h). The amount of Lz adsorbed was calculated by subtracting the amount found in the supernatant liquid after adsorption from the amount of Lz present before addition of the adsorbent by UV absorption at 281.5 nm. Calibration experiments were done separately before each set of measurements with lysozyme solutions of different concentrations buffered at the same pH as the isotherm. Centrifugation prior to the analysis was used to avoid potential interference from suspended scattering particles in the UV−vis analysis.

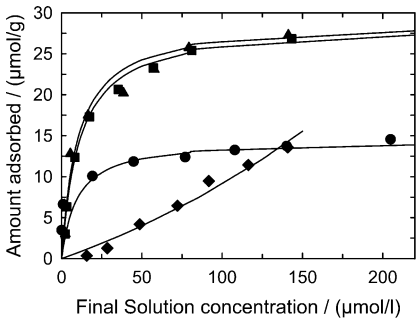

Figure 1. Adsorption isotherm of Lz on C_{16}-MCM-41 at various pH values: (●) 6.5, (■) 9.6, (▲) 10.5, and (◆) 12.0.

TABLE 1: Textural Parameters of the Pure Silica and Aluminum-Containing Mesoporous Molecular Sieves Employed in This Study

sample	a_0, nm	A_{BET}, m^2/g	pore vol, cm^3/g	$d_{p,NLDFT}$, nm
C_{12}-AlMCM-41	3.47	1024	0.57	3.2
C_{12}-MCM-41	3.54	1212	0.70	3.1
C_{16}-AlMCM-41	4.15	1105	0.79	3.8
C_{16}-MCM-41	4.10	1135	0.86	3.9
AlSBA-15	11.76	604	1.26	9.1
SBA-15	10.89	910	1.25	8.8

Results and Discussion

The textural properties of the pure silica and aluminum-substituted C_n-MCM-41 and materials are collected in Table 1. All materials under investigation possess a surface area of ca. 1000 m^2/g and a pore diameter exceeding 3 nm. The pore volume ranges from 0.57 (C_{12}-MCM-41) to 1.26 cm^3/g (AlSBA-15). The detailed characterization of the materials employed in this study is reported elsewhere.[45]

The adsorption isotherms of lysozyme (Lz) on MCM-41 at different solution pH ranging from 6.5 to 12 are shown in Figure 1. The isotherms measured in the pH range 6.5 to 10.5 show a sharp initial rise, suggesting a high affinity between Lz and the adsorbent surface. Finally, the isotherms reach a plateau (type L (Langmuir) isotherm). The solid lines in this figure represent a fit of the experimental data employing the Langmuir model. The monolayer adsorption capacity was calculated by using the Langmuir equation

$$n_s = Kn_m c/(1 + Kc)$$

where K is the Langmuir constant, c is the lysozyme concentration, n_m is the monolayer adsorption capacity, and n_s is the amount of Lz adsorbed on the adsorbent. The isotherm measured at pH 12.0 represents a type S isotherm and the solid line is a fit of the experimental data employing the BET model. The monolayer adsorption capacity was calculated by using the simplified form of BET equation,

$$n_s = Cn_m c/\{(1 - c)(1 + (C - 1)c)\}$$

where C is the BET constant, c is the concentration of Lz, n_m is monolayer adsorption capacity, and n_s is the amount of Lz adsorbed on the adsorbent.

The maximal amount of Lz adsorbed n_m (determined from the Langmuir or BET fit) also significantly changes with the

solution pH. The amount adsorbed increases from pH 6.5 to 10.5 and decreases when the pH is increased to 12. The maximum adsorption of Lz amounts to 28.1 μmol/g at a pH of 10.5, while only 14.0 μmol/g are adsorbed at pH 6.5. It is interesting to note that the monolayer adsorption capacity at pH 10.5 is almost twice the amount of the Lz adsorbed at pH 6.5. The isoelectric point pI of Lz is around 11,[33] and, hence, the protein is positively charged at a pH below pI and negatively charged at a pH above pI. The isoelectric point of the silica surface of MCM-41 is around 3.6,[46] and, hence, the adsorbent is negatively charged at a pH above 3.6. It has been reported that the net positive charge of the Lz molecule increases from 8 at pH 8 to 10 at pH 4.[47] The above results suggest that the electrostatic attraction between Lz and the silica surface should increase with decreasing solution pH. In contrast, the monolayer adsorption capacity decreases with decreasing solution pH. This indicates that the lateral repulsion between the protein molecules is more significant at lower solution pH than the electrostatic interaction between the negatively charged silica surface and the positively charged lysine and arginine amino acid residues on the protein surface. This behavior can also be explained by the change of the limiting area per molecule for Lz with solution pH. It has been reported that the area per molecule of Lz in solution having a pH near the isoelectric point is similar to the area per molecule of Lz in its crystallized state (13.5 nm^2), whereas it is 26.6 nm^2 at a solution pH of 4.[47] This could be due to an increase of the number of positive charges on the protein below the isoelectric point. Therefore, at a solution pH of 6.5, the Lz molecules are larger and occupy more space than in a solution with a pH near the pI. In turn, a reduced net limiting area per Lz molecule leads to a denser packing of the adsorbed lysozyme molecules. In addition, hydrophobic interactions are more dominant near the pI than electrostatic interactions. These hydrophobic interactions originate from (1) the interaction between the nonpolar side chains of the amino acids residues on the surface of Lz and surface siloxane bridges or (2) from the Lz−Lz interactions between the hydrophobic side chains of neighboring Lz molecules adsorbed on the surface of MCM-41. Moreover, the buffer used (phosphate vs bicarbonate) might also effect the lysozyme adsorption.[39] Ball et al. also found that lysozyme adsorption increases with pH (from 4.5 to 8.9) at a silica−titania surface.[41] They ascribed the observed behavior to differences in the adsorption mechanism. At high pH, where the enzyme aggregates in solution, the enzyme adsorbs in a biphasic reaction, while it adsorbs as monomers at acidic pH.[41] Whether the observed increase in adsorption with increasing pH observed in this study can also be explained by self-association is at present unclear and subject to further studies.

It is interesting to note that the amounts of lysozyme adsorbed at pH 9.6 and 10.5 do not differ very much. The external surface of Lz is covered with lysine and arginine amino acid residues. The pI of lysine is 9.59 and the pI of arginine is around 11. Hence, the positive charge on the external surface of Lz near pH 9.6 is similar to that for pH 10.5. Therefore, the amount adsorbed is almost as similar at pH 9.6 and 10.5. It should also be noted that the form of the adsorption isotherm measured at a solution pH of 12.0 is completely different from the isotherms measured at pH values ranging from 6.5 to 10.5. The isotherm measured at pH 12.0 is a type S isotherm, which indicates that the interaction between lysozyme molecule and the silica surface is week compared to the interaction between two Lz molecules. Both the surface of the protein molecule and the silica surface are negatively charged, which creates a strong repulsion and leads to a low amount of adsorption. However, the amount

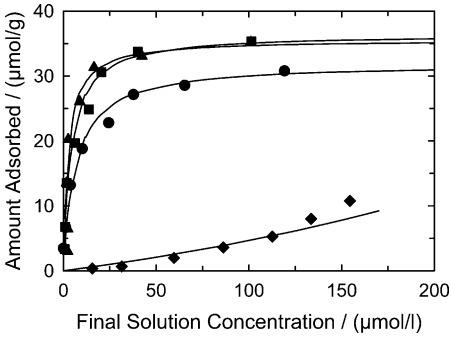

Figure 2. Adsorption isotherm of Lz on SBA-15 at various pH values: (●) 6.5, (■) 9.6, (▲) 10.5, and (◆) 12.0.

TABLE 2: Comparison of the Amount of Lz Adsorbed onto C_{16}-MCM-41 in This Work with Previously Reported Data

solution pH	final solution concn, μmol/L	contact time, h	loading, μmol/g	ref
6.0[a]	35	96	10.2	42
6.0[a]	45	96	10.5	42
6.5[b]	45	96	12.0	this work
6.5[b]	200	96	14.6	this work
10.6[b]	45	96	23.8	this work
10.6[b]	141	96	28.1	this work

adsorbed increases with increasing bulk Lz solution concentration indicating that the lateral interaction between the protein molecules promotes the adsorption of further Lz molecules after the adsorption of some Lz molecules on the surface. It also has been reported earlier[39] that lysozyme hardly adsorbs under conditions of electrostatic repulsion at hydrophobic surfaces, which is in line with our findings.

Table 2 compares the observed Lz loadings on C_{16}-MCM-41 at different pH values as a function of the final solution concentration in this work with previously published data by Kisler et al.[42] The amount of Lz adsorbed in the final solution concentration around 45 μmol/g is 12.0 and 10.5 for this work and the work of Kisler et al.,[42] respectively. However, we measured the adsorption isotherm up to a final solution concentration of 200 μmol/g resulting in an amount adsorbed of 14.6 μmol/g. This suggests that the saturation level is not reached at the initial concentration studied in the work of Kisler et al.[39] However, in agreement with the previously published data, we also found that 72 to 96 h are needed to establish thermodynamic equilibrium in our adsorption experiments (the adsorption kinetics of C_{16}-MCM-41 and SBA-15 at pH 10.5 are presented in the Supporting Information.). Moreover, at a pH of 10.5 (final solution concentration of 45 μmol/L), we observed a more than two times higher Lz adsorption (23.8 μmol/g) than the one reported at a solution pH of 6.0.[42] Hence, we concluded that a pH close to the pI of Lz is beneficial for adsorption and separation processes provided that both the protein and the adsorbent are stable under these conditions.

Figure 2 shows the adsorption isotherms of Lz adsorbed onto SBA-15 at different solution pH values ranging from 6.5 to 12. The amount of Lz adsorbed at a solution pH of 9.6 and 10.5 is 36.0 and 35.3 μmol/g, respectively, while 31.3 μmol/g of Lz is adsorbed at a solution pH of 6.5. The difference between the amount adsorbed at a solution pH of 10.5 and 6.5 for SBA-15 is only 4 μmol/g whereas a difference of 14 μmol/g is observed for C_{16}-MCM-41. It is well-known that the size of protein molecules is larger at a pH below the pI and, thus, the protein size and the pore diameter of MCM-41 are similar. Therefore, the Lz molecules may block the pores entrances of MCM-41 and may not allow other Lz molecules to penetrate inside. As

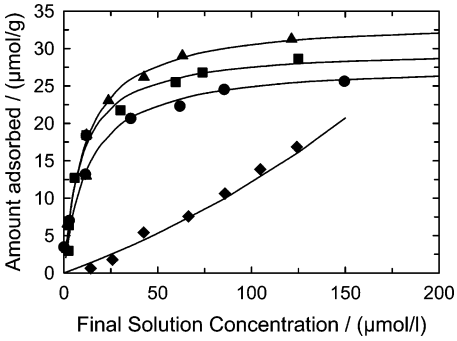

Figure 3. Adsorption isotherm of Lz on C_{16}-AlMCM-41 at various pH values: (●) 6.5, (■) 9.6, (▲) 10.5, and (◆) 12.0.

a consequence, part of the inner pore surface remains inaccessible leading to lower adsorption.[45] In the case of SBA-15, the pore diameter is more than two times larger than the size of the Lz molecule and pore blocking can be ruled out. At pH 12 also an S-type isotherm is observed, which confirms that the repulsion between the negatively charged surface and the protein molecule dominates.

Figure 3 shows the adsorption isotherms of Lz adsorbed onto C_{16}-AlMCM-41 ($n_{Si}/n_{Al} = 23$) at different solution pH. The monolayer adsorption capacity (determined from the Langmuir fit) increases from 26.8 to 32.6 μmol/g in the range of pH 6.5 to 10.5. Thereafter, the adsorption capacity is drastically reduced from 32.6 to 20.6 μmol/g at the solution pH of 12.0. At a pH near the isoelectric point, the net charge of the protein is zero and hence the lateral interactions between the protein molecules are reduced. Moreover, even when the overall charge on the protein is zero, the charge and hydrophobicity within each domain of the protein may be different[48] and the negatively charged aluminosilicate surface may attract the polar and positively charged regions of the Lz molecules, thus leading to higher amount of adsorption at a solution pH close to the pI. The low monolayer adsorption capacity at a solution pH of 12.0 is due to the strong electrostatic repulsion between the protein and the adsorbent surface.

The comparison of the monolayer adsorption capacity of pure silica C_{16}-MCM-41 and C_{16}-AlMCM-41 ($n_{Si}/n_{Al} = 23$) as a function of solution pH is shown in Figure 4a. The pH dependence of the adsorption of globular proteins on different substrates has been discussed by Su et al.[47] The adsorption capacities are normally found to be bell-shaped with respect to pH variation with the peak located in the region of the isoelectric point. A similar behavior is observed in our systems. The amount adsorbed is always higher for AlMCM-41 as compared to MCM-41 irrespective of the solution pH.

A maximum monolayer adsorption capacity of 47.2 μmol/g was observed for AlSBA-15 ($n_{Si}/n_{Al} = 7$) at a solution pH of 9.6 whereas only 43.3 μmol/g was adsorbed at the solution pH of 10.5 (Figure 4b). The reason for the observed shift of the adsorption maximum from pH 10.5 to 9.6 is at present unknown. It has been reported by Haynes and Norde[49] that the maximal amount of adsorbed peaks occurs at the isoelectric point of the protein/substrate complex and not at the pI of the bulk solution. The reason for this behavior is that on contact the negative charges on the adsorbent surface neutralize some of the positively charged groups on the protein, causing a shift of the bulk solution isoelectric point to a lower pH. However, apossible explanation is the higher Al content of AlSBA-15 ($n_{Si}/n_{Al} = 7$) as compared to C_{16}-AlMCM-41 ($n_{Si}/n_{Al} = 23$) resulting in a higher number of negative charges. Therefore, the increase in the number of negative charges on the surface of AlSBA-15

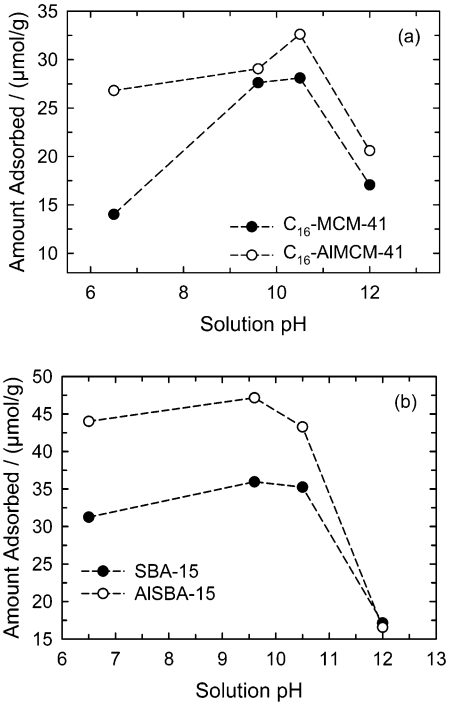

Figure 4. Comparison of the maximum amount adsorbed of Lz as a function of solution pH on (a) C_{16}-MCM-41 and C_{16}-AlMCM-41 and (b) SBA-15 and AlSBA-15.

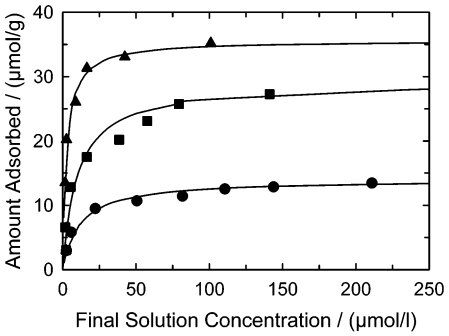

Figure 5. Comparison of the adsorption isotherm of Lz on mesoporous adsorbents with various pore diameters at pH 10.5: (▲) SBA-15, (■) C_{16}-MCM-41, and (●) C_{12}-MCM-41.

due to a higher number of Al atoms might shift the pI of the Lz solution to lower pH, which results in an increase in the number of positive charges on the surface of the protein. This would enhance the interaction with the negatively charged aluminosilicate surface resulting in a higher amount of Lz adsorption at a solution pH of 9.6. The adsorption of Lz on AlSBA-15 is higher irrespective of the solution pH (except at pH 12.0) in comparison to all other adsorbents employed in the present study.

Figure 5 compares the adsorption isotherms of Lz adsorbed on pure silica mesoporous adsorbents such as C_{12}-MCM-41, C_{16}-MCM-41, and SBA-15 at a solution pH of 10.5. The monolayer adsorption capacity increases with increasing pore volume and pore diameter of the mesoporous adsorbent. It can be seen from Table 1 that pore volume and pore diameter decrease in the following order: SBA-15 > C_{16}-MCM-41 > C_{12}-MCM-41. The maximal monolayer adsorption capacity of C_{12}-MCM-41 is 13.4 μmol/g, whereas 28.1 and 35.3 μmol/g were observed for C_{16}MCM-41 and SBA-15, respectively. It should be noted that the volumes occupied by the Lz molecule ($V = 17.8$ nm^3) are 20.1% and 35.1% of the specific pore volumes of the C_{12}-MCM-41 and C_{16}-MCM-41 determined by

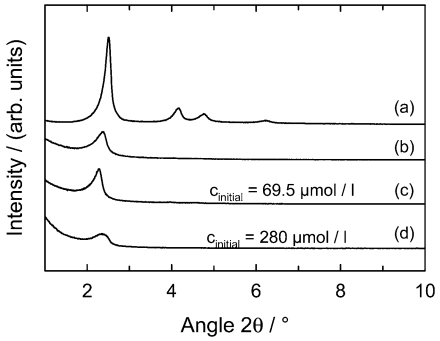

Figure 6. XRD powder patterns of C_{16}-MCM-41 before and after Lz adsorption at pH 10.5: (a) C_{16}-MCM-41, (b) C16MCM-41 after immersing in a buffer solution for 96 h, (c) C_{16}-MCM-41(69.5 μmol/L), and (d) C_{16}-MCM-41(280 μmol/L).

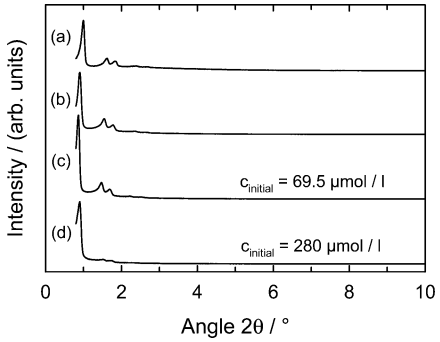

Figure 7. XRD powder patterns of SBA-15 before and after Lz adsorption at pH 10.5: (a) SBA-15, (b) SBA-15 after immersing in a buffer solution for 96 h, (c) SBA-15(69.5 μmol/L), and (d) SBA-15-(280 μmol/L).

nitrogen adsorption, respectively, whereas only 30.3% of the specific pore volume was occupied in the large pore SBA-15 adsorbent. This could be due to the presence of (ultra)micropores in SBA-15 which are not even accessible for small molecules such as benzene and cyclohexane.[50] The low adsorption capacity of C_{12}-MCM-41 as compared to the other adsorbents with larger pore diameter could be due its pore size, which is similar to the size of Lz molecule. Hence, it is possible that some pores are not accessible for Lz adsorption due to their small pore opening.

Characterization of the Adsorbent after Adsorption. An important question that needs to be addressed is whether the protein is adsorbed in the pores of the adsorbent or merely to the external surface of the particles. A feasible method to address this question is the analysis of the adsorbent before and after adsorption by XRD and nitrogen physisorption to indicate the stability of the adsorbent and the extent of pore filling.

Figures 6 and 7 show the powder XRD patterns of C_{16}-MCM-41 and SBA-15 before and after adsorption of lysozyme at two different initial Lz concentrations (69.5 and 280 μmol/L) at pH 10.5 in comparison to the XRD pattern of MCM-41 prior to protein adsorption and after stirring for 96 h in the buffer solution (pH 10.5). A strong decrease in XRD peak intensity is observed after Lz adsorption onto C_{16}-MCM-41 (Figure 6), as well as after stirring the adsorbent in the buffer solution at pH 6.5. In the case of SBA-15 (Figure 7) all samples exhibit a prominent peak in the diffraction pattern at $2\theta \approx 1°$ and two small peaks at higher angle. The observation of at least three reflections after loading with Lz at pH 10.5 is consistent with the retention of the hexagonal mesoporous structure. As shown above, the amount adsorbed increases with the initial Lz concentration. The intensity of the low-angle (100) and high-angle peaks (110 and 200) decreases as compared to the parent SBA-15 materials with increasing Lz concentration in the solution. This cannot be interpreted as a severe loss of structural order, but it is likely that larger contrast in density between the silica walls and the open pores relative to that between the silica walls and the Lz molecule is responsible for the observed decrease in intensity.[51,52] This effect is even more prominent when a higher initial Lz concentration is used, which results in a higher Lz loading. This indicates that Lz molecules can be packed inside the mesopores without affecting the structural integrity of the parent SBA-15 materials.

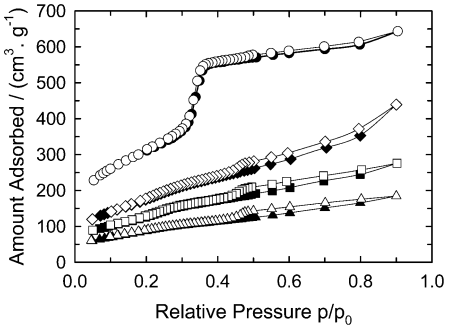

Figure 8. Nitrogen adsorption isotherms of C_{16}-MCM-41 before and after Lz adsorption at pH 10.5 (open symbols, adsorption; closed symbols, desorption): (○) C_{16}-MCM-41, (◇) C_{16}-MCM-41 after immersing in a buffer solution for 96 h, (□) C_{16}-MCM-41(69.5 μmol/L), and (△) C_{16}-MCM-41(280 μmol/L), where 69.5 and 280 μmol/L are the initial Lz concentrations.

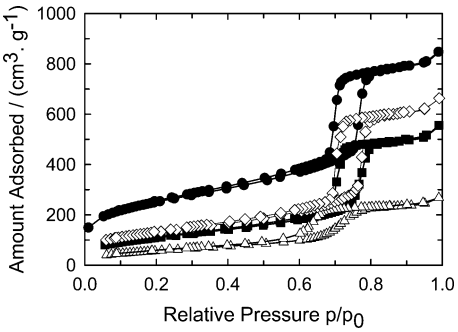

Figure 9. Nitrogen adsorption isotherms of SBA-15 before and after Lz adsorption at pH 10.5: (●) SBA-15, (◇) SBA-15 after immersing in a buffer solution for 96 h, (■) SBA-15 (69.5 μmol/L), and (△) SBA-15 (280 μmol/L), where 69.5 and 280 mmol/L are the initial Lz concentrations.

The N_2 adsorption isotherms of C_{16}-MCM-41 and SBA-15 before and after loading with different amounts of Lz (69.5 and 280 μmol/g initial concentration) are shown in Figures 8 and 9, respectively. The amount of nitrogen adsorbed decreases markedly with lysozyme adsorption, but did not decrease as much after buffer contact in the absence of the protein. Similar results have been observed for the adsorption of lysozyme onto MCM-41 at a pH of 6.5.[22] In the case of SBA-15, even after adsorption the samples exhibit a type 1V isotherm with a broad hysteresis loop that is typical for large-pore mesoporous materials. However, the isotherms observed for C_{16}-MCM-41 after Lz adsorption are more of type II of the IUPAC classification, which indicates that the mesopores are filled with Lz molecules (and water).

Table 3 summarizes the textural properties of C_{16}-MCM-41 and SBA-15 samples loaded with lysozyme at pH 10.5. The mesopore volume and the surface area are drastically reduced after the adsorbent is stirred in the buffer solution and after lysozyme adsorption.

TABLE 3: Textural Properties of C_{16}-MCM-41 and SBA-15 Samples Loaded with Different Amounts of Lysozyme at pH 10.5 and after Stirring in a Buffer Solution at the Same pH for 96 h

sample	initial concn, μmol/L	loading, μmol/g	A_{BET}, m^2/g	V_p, cm^3/g	Lz_{area}, m^2/g	Lz_{vol}, cm^3/g
SBA-15	69.5	13.5	403	0.79	110	0.15
SBA-15	280	35.3	211	0.38	287	0.38
SBA-15 (buffer soln)			479	0.95		
C_{16}-MCM-41	69.5	12.8	442	0.27	104	0.14
C_{16}-MCM-41	280	28.1	326	0.18	229	0.30
C_{16}-MCM-41 (buffer soln)			659	0.37		

Although a reduction of surface area and pore volume is observed after 96 h of stirring in a buffer solution at pH 10.5, the large reduction in the specific pore volume and the specific surface area are tentatively attributed to the tight packing of the Lz molecule in the mesopores of C_{16}-MCM-41. Moreover, it is interesting to note that the actual volume of the Lz adsorbed (28.1 μmol/g) in the pores of MCM-41 is only 0.30 cm^3/g (assuming that the net volume of one Lz molecule is 1.78×10^{-20} cm^3), which is 35.1.8% of the total free volume of the C_{16}-MCM-41 material, while the nitrogen adsorption measurement shows 79.1% reduction in the specific pore volume of C_{16}-MCM-41. Moreover, the actual net surface area occupied by the Lz (28.1 μmol/g) adsorbed is only 228.5 m^2/g (assuming that the net area of one Lz molecule is 1.35 nm^2), which is only 20.1% of the specific surface area of C_{16}-MCM-41 materials before adsorption. This large discrepancy in the surface area and pore volume indicates that the Lz molecules (3.0×4.5 nm) are filling the MCM-41 pore system in such a way that the adsorption of nitrogen is hindered.

After loading 35.3 μmol/g of Lz in SBA-15, the surface area is reduced from 910 to 211 m^2/g, which is a 76.8% reduction of the total specific surface area. The pore volume is reduced from 1.25 to 0.38 cm^3/g, which is 69.6% reduction of the specific pore volume of parent SBA-15. The net surface area and total volume of the Lz molecule adsorbed on the pores of SBA-15 are 287 m^2/g and 0.38 cm^3/g, respectively, which are only 31.5% and 30.4% of the total specific surface area and the specific pore volume of SBA-15 material before adsorption. Although the monolayer adsorption capacity of SBA-15 is higher as compared with the C_{16}-MCM-41, the reduction in the specific pore volume is lower after adsorption. This could be a consequence of the large pore size of SBA-15 material, which might allow access of nitrogen molecules even after the adsorption of Lz. In addition, it is well-known that SBA-15 contains a high amount of (ultra)micropores which are not even accessible for small molecules such as cyclohexane and benzene.[50]

Table 4 summarizes the textural properties of MCM-41 and SBA-15 materials after Lz adsorption at different solution pH, using an initial Lz concentration of 69.5 μmol/g. The results reveal a reduction in specific surface area and pore volume, which shows that the protein adsorption occurs predominately inside the mesopores of the material. The reduction of specific surface area and specific pore volume observed for C_{12}- and C_{16}-MCM-41 is less at pH 6.5 as compared with pH 9.6 and 10.5, which is in line with the increase in monolayer adsorption capacity found. As discussed above, the size of the Lz molecule increases with decreasing pH because of the strong electrostatic repulsion between the amino acids present in the molecule. N_2 adsorption results show that at a pH of 6.5, the specific pore volume is reduced by 50% and 61.6% for C_{12}-MCM-41 and C_{16}-MCM-41, respectively, while the reduction amounts to 65.7% and 68.6% at a solution pH of 10.5. Assuming a Lz volume of 17.8 cm^3, the Lz molecules occupied only 6.5% and 12.6% of the total free volume of C_{12}- and C_{16}-MCM-41, respectively, at a solution pH of 6.5, and the occupied volume increased to 14.5% and 16.0% of the total free value at a solution pH of 10.5, using initial Lz concentrations of ca. 69.5 μmol/g, which is well below the saturation limit. Moreover, the instability of MCM-41 toward water increases with increasing pH due to hydrolysis of Si−O−Si bonds.[53] While immersing MCM-41 into a buffer solution at pH 6 for 48 h does not result in a significant decrease in nitrogen adsorption capacity,[22] conducting the same experiment in a buffer solution at pH 10.5 does result in a significant reduction of the nitrogen adsorption (cf. Figure 8). It is therefore clear that the adsorption of lysozyme on MCM-41 at higher pH is hampered by a slow hydrolysis of the adsorbent.

TABLE 4: Textural Parameters of MCM-41 and SBA-15 Materials after Lz Adsorption at Different Solution pH, Using an Initial Lz Concentration of 69.5 μmol/L

	C_{12}-MCM-41		C_{16}-MCM-41		SBA-15	
soln pH	A_{BET}, m^2/g	V_p, cm^3/g	A_{BET}, m^2/g	V_p, cm^3/g	A_{BET}, m^2/g	V_p, cm^3/g
6.5	771	0.35	552	0.33	412	0.80
9.6	457	0.24	438	0.27	347	0.73
10.5	467	0.25	442	0.27	403	0.79
12.0	197	0.11	253	0.14	399	0.86

It should also be noted that the Lz volume is calculated from crystallographic data and so the dimensions in solution and the adsorbed state may differ from the crystallographic dimension (3.0×4.5 nm^2). Moreover, lysozyme undergoes significant changes in size depending on solution pH. Finally, due to repulsion between the adsorbed molecules, the space required for an adsorbed molecule is significantly more than its crystallographic size. Therefore, the large difference in occupied pore volume between the theoretical and the experimental value obtained from the N_2 adsorption is not surprising. Lz molecules might also block the mesopores entrance excluding the adsorption of nitrogen molecule as the pore size of Lz is similar to the pore size of C_{12}- and C_{16}-MCM-41 materials. In the case of SBA-15, only 30.2% and 30.9% of the total pore volume were occupied by Lz at a solution pH of 6.5 and 10.5, respectively, while 34.9% was occupied at a pH of 9.6. These results also show that the stability of pure silica SBA-15 toward water is significantly higher as compared to that of MCM-41, probably due to the higher wall thickness (2−3 nm).[21] Therefore, both the higher pore volume (and diameter) and the higher stability render SBA-15 a superior adsorbent compared to MCM-41.

To check the structural stability of Lz after adsorption on the mesoporous supports, diffuse reflectance Fourier transform infrared (DRIFT) spectra were recorded for the Lz loaded mesoporous adsorbents SBA-15 and C_{16}-MCM-41 in comparison to pure lysozyme. Figure 10 shows the typical DRIFT spectrum for lysozyme recorded at room temperature. There are nine normal modes which are allowed for the amide band of proteins. These are called A, B, and I to VII in order of decreasing frequency. The amide bands I−III are generally employed to study the protein structure. The amide band I (near 1650 cm^{-1}) is due to the C═O stretching mode, whereas the amide II band (near 1550 cm^{-1}) is due to the bending and the stretching mode of N−H and C−N vibrations, respectively. Typically, the disappearance of the amide II N−H stretching mode is used to follow the unfolding of the protein. The amide band III (near 1300 cm^{-1}) is due to the stretching and bending

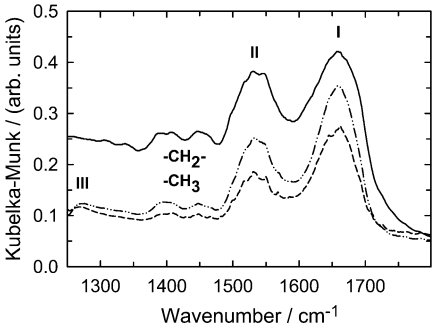

Figure 10. Comparison of the DRIFT spectra of pure Lz and different amounts of Lz loaded on C_{16}-MCM-41 materials: (—) Lz, (—••—) C_{16}-MCM-41(280 μmol/L), and (- - -) C_{16}-MCM-41(69.5 μmol/L), where 280 and 69.5 μmol/L are the initial Lz concentrations.

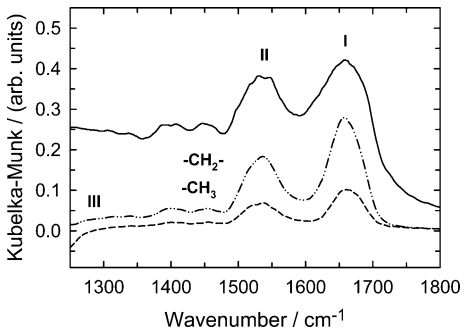

Figure 11. Comparison of the DRIFT spectra of pure Lz and different amounts of Lz loaded on SBA-15 materials: (—) Lz, (—••—) SBA-15(280 μmol/L), and (- - -) SBA-15 (69.5 μmol/L), where 280 and 69.5 μmol/L are the initial Lz concentrations.

mode of C−N and N−H.[51] The DRIFT spectrum of lysozyme (Figure 10) shows five main bands centered at 1653, 1533, 1446, 1384, and 1252 cm^{-1}. It has been reported that proteins having a α-helical conformation show strong amide I bands between 1650 and 1655 cm^{-1}. Thus the band observed at 1653 cm^{-1} is due to the α-helical confirmation of the Lz molecule. The strong amide II band at 1533 cm^{-1} is due to the parallel β-sheet structure of Lz.[54] It is important to note that this band is used in assigning random structure and in accurate estimation of helix and random components.[54] The bands near 1446 and 1384 cm^{-1} are assigned to the CH_2 and CH_3 stretching modes of the aliphatic moieties of amino acid side chains. The band at 1252 cm^{-1} (amide III band) can also be assigned to β-sheets.[55] However, the amide III band is a very complex band and depends on the force field, the nature of the side chains, and hydrogen bonding. Therefore, this band is only of limited use for the extraction of structural information.

Figures 10 and 11 also show the DRIFT spectrum of Lz adsorbed on C_{16}-MCM-41 and SBA-15, respectively, after subtraction of the spectrum of unloaded C_{16}-MCM-41 or SBA-15. The spectra also show all five major bands centered at 1653, 1533, 1446, 1384, and 1252 cm^{-1}. The intensities of the amide I and II bands clearly indicate that the structural confirmation of Lz is retained after adsorption on SBA-15 and C_{16}-MCM-4. It can be assumed that the Lz molecules are tightly packed inside the mesopores of both materials and do not have room for changing their structural confirmation inside the mesoporous matrix. Moreover, the intensities of all five peaks in the 1700−1200 cm^{-1}region increase with increasing Lz loading on both SBA-15 and C_{16}-MCM-41. This also confirms that the adsorption of Lz onto the mesoporous supports does not lead to a denaturation of the protein.

Conclusions

Adsorption of lysozyme over mesoporous materials such as MCM-41, AlMCM-41, SBA-15, and AlSBA-15 has been studied from lysozyme solutions with different pH. It has been found that the amount of lysozyme adsorbed depends on the solution pH as well as the specific pore volume and the composition of the adsorbent. The maximum amount of lysozyme has been achieved for AlSBA-15 at solution pH 9.6 and amounted to 47.2 μmol/g (ca. 680 mg/g). This may due to the zero net charge of the lysozyme molecule at this pH, and so there is no electrostatic repulsion or attraction between the amino acids, resulting in a size reduction of the lysozyme molecule. The influence of specific pore volume on the adsorption of lysozyme also has been studied by using adsorbents with different pore diameter. It has been found that the amount adsorbed is mainly a function of the specific pore volume. N_2 adsorption and XRD data after lysozyme adsorption reveal that the lysozyme molecule is adsorbed inside the channels of mesoporous adsorbents. The stability of SBA-15 toward the buffer solution is higher for SBA-15 as compared to MCM-41, which is probably a consequence of the higher wall thickness of the former material. DRIFT spectra of the adsorbed lysozyme confirm that the adsorption of the enzyme did not result in denaturation of Lz.

Acknowledgment. Financial support of this work by Fonds der Chemischen Industrie is gratefully acknowledged.

Supporting Information Available: Lysozyme adsorption kinetics on C_{16}-MCM-41 and SBA-15 at pH 10.5 (Figure S1). This material is available free of charge via the Internet at http://pubs.acs.org.

References and Notes

(1) *Proteins at Interfaces II*: *Fundamentals and Applications*; Horbett, T. A., Brash, J. L., Eds.; American Chemical Society: Washington, DC, 1995.

(2) *Proteins at Interfaces*: *Physicochemical and Biochemical Studies*; Brash, J. L., Horbett, T. A., Eds.; American Chemical Society: Washington, DC, 1987.

(3) Andrade, J. D.; Hlady, V. *Adv. Polym. Sci.* **1986**, *79*, 1.

(4) Sandu, C.; Singh, R. K. *Food Technol.* **1991**, *45*, 84.

(5) Hubbell, J. A. *Bio/Technol.* **1995**, *13*, 565.

(6) Ishihara, K.; Oshida, H.; Endo, Y.; Ueda, T.; Watanabe, A.; Nakabayashi, N. *J. Biomed. Mater. Res.* **1992**, *26*, 1543.

(7) Feng, M.; Morales, A. B.; Beugeling, T.; Bantjes, A.; Vanderwerf, K.; Gosselink, G.; Degrooth, B.; Greve, J. *J. Colloid Interface Sci.* **1996**, *177*, 364.

(8) Klibanov, A. M. *Science* **1983**, *219*, 722.

(9) Rechnitz, G. A. *Chem. Eng. News* **1998**, *66*, 24.

(10) Martin, B. D.; Gaber, B. P.; Patterson, C. H.; Turner, D. C. *Langmuir* **1998**, *14*, 3971.

(11) Inglis, W.; Sanders, G. H.; Williamsan, P. M.; Davies, M. C.; Roberts, C. J.; Tendler, S. J. B. *Langmuir* **2001**, *17*, 7402.

(12) Weetall, H. H. *Appl. Biochem. Biotechnol.* **1993**, *41*, 157.

(13) Avnir, D.; Braun, S.; Lev, O.; Ottolenghi, M. *Chem. Mater*. **1994**, *6*, 1605.

(14) Dave, B. C.; Dunn, B.; Valentine, J. S.; Zink, J. I. *Anal. Chem.* **1994**, *66*, 1120A.

(15) Weetall, H. H. *Analtical Uses of Immobilized Biological Compounds for Detection, Medical and Industrial Uses*; Guilbault, G. G., Mascini, M., Eds.: D. Reidel Publishing Co.: Boston; MA, 1988; p 1.

(16) Kresge, C. T.; Leonowicz, M. E.; Roth, W. J.; Vartuli, J. C.; Beck, J. S. *Nature* **1992**, *359*, 710.

(17) Zhao, D.; Huo, Q.; Feng, J.; Chmelka, B. F.; Stucky, G. D. *J. Am. Chem. Soc.* **1998**, *120*, 6024.

(18) (a) Zhao, D.; Feng, J.; Huo, Q.; Melosh, N.; Fredrikson, G.; Chmelka, B.; Stucky, G. D. *Science* **1998**, *279*, 548. (b) Yang, P.; Zhao, D.; Margolese, D.; Chmelka, B.; Stucky, G. D. *Nature* **1998**, *396*, 152.

(19) Corma, A.; Navarro, M. T.; Pariente, J. P. *J. Chem. Soc., Chem. Commun.* **1994**, 147.

(20) Luan, Z.; Kevan, L. *J. Phys. Chem. B* **1997**, *101*, 2020.

(21) Reddy, K. M.; Moudrakovski, I.; Sayari, A. *J. Chem. Soc., Chem. Commun.* **1994**, 1059.
(22) Daehler, A.; Stevens, G. W.; O'Connor, A. In *Nanoporous Materials−Science and Engineering*; Lu, G. Q (Max), Zhao, X. S., Eds.; Imperial College Press: in press.
(23) Diaz, J. F.; Balkus, K. J. *J. Mol. Catal. B*: *Enzymatic* **1996**, *2*, 115.
(24) (a) Yiu, H. H. P.; Wright, P. A.; Botting, N. P. *Microporous Mesoporous Mater.* **2001**, *44−45*, *763*. (b) Yiu, H. H. P.; Wright, P. A.; Botting, N. P. *J. Mol. Catal. B*: *Enzymatic* **2001**, *15*, 81.
(25) (a) Deere, J.; Magner, E.; Wall, J. G.; Hodnett, B. K. *Chem. Commun*. **2001**, 465. (b) Deere, J.; Magner, E.; Wall, J. G.; Hodnett, B. K. *Catal. Lett*. **2003**, *85*, 19.
(26) Han, Y.-J.; Watson, J. T.; Stucky, G. D.; Butler, A. *J. Mol. Catal. B*: *Enzymatic* **2002**, *17*, 1.
(27) Takahashi, H.; Li, B.; Sasaki, T.; Miyazaki, C.; Kajino, T.; Inagaki, S. *Microporous Mesoporous Mater.* **2001**, *44−45*, *755*.
(28) Gomez, J. M.; Deere, J.; Goradia, D.; Cooney, J.; Magner, E.; Hodnett, B. K. *Catal. Lett*. **2003**, *88*, 183.
(29) Blake, C. C. F.; Koenig, D. F.; Mair, G. A.; North, A. C. T.; Phillips, D. C.; Sarma, V. R. *Nature* **1965**, *206*, 757.
(30) Garrett, Q.; Garrett, R. W.; Milthorpe, B. K. *Invest. Ophthalmol. Visual Sci.* **1999**, *40*, 897.
(31) Canfield, R. E.; Liu, A. K. *J. Biol. Chem.* **1965**, *240*, 2000.
(32) Kharakoz, D. P.; Sarvazyan, A. P. *Biopolymers* **1993**, *33*, 11.
(33) Wilson, K. P.; Malcolm, B. A.; Matthews, B. W. *J. Biol. Chem.* **1992**, *267*, 10842.
(34) Bell, J. A.; Wilson, K. P.; Zhang, X. J.; Faber, H. R.; Nicholson, H.; Matthews, B. W. *Proteins* **1991**, *10*, 10.
(35) Wahlgren, M.; Arnebrant, T.; Lundström, I. *J. Colloid Interface Sci.* **1995**, *175*, 506.
(36) Su, T. J.; Lu, J. R.; Thomas, R. K.; Cui, Z. F.; Penfold, J. *J. Colloid Interface Sci*. **1998**, *203*, 419.
(37) Robeson, J. L.; Tilton, R. D. *Langmuir* **1996**, *12*, 6104.
(38) Norde, W.; Anusiem, A. *Colloids Surf.* **1992**, *66*, 73.
(39) Ball, V.; Ramsden, J. J. *J. Phys. Chem. B* **1997**, *101*, 5465.
(40) Ball, V.; Ramsden, J. J. *Phys. Chem. Chem. Phys*. **1999**, *1*, 3667.
(41) Ball, V.; Ramsden, J. J. *Colloids Surf. B* **2000**, *17*, 81.
(42) Kisler, J. M.; Dähler, A.; Stevens, G. W.; O'Connor, A. J. *Microporous Mesoporous Mater.* **2001**, *44−45*, 769.
(43) Kisler, J. M.; Stevens, G. W.; O'Connor, A. J. *Mater. Phys. Mech.* **2001**, *4*, 89.
(44) Hartmann, M.; Raccouchot, S.; Bischof, C. *Microporous Mesoporous Mater*. **1999**, *27*, 309.
(45) Vinu, A.; Murugesan, V.; Tangermann, O.; Hartmann, M. Submitted for publication.
(46) Deere, J.; Magner, E.; Wall, J. G.; Hodnett, B. K. *J. Phys. Chem. B* **2002**, *106*, 7340.
(47) Su, T. J.; Lu, J. R.; Thomas, R. K.; Cui, Z. F.; Penfold, J. *Langmuir* **1998**, *14*, 438.
(48) Peters, T. *Adv. Protein Chem.* **1985**, *37*, 161.
(49) Haynes, C. A.; Norde, W. *Colloids Surf. B* **1994**, *2*, 517.
(50) Hartmann, M.; Bischof, C. *Prepr. Am. Chem. Soc., Div. Pet. Chem.* **2001**, *46*, 23.
(51) Hammond, W.; Prouzet, E.; Mahanti, S. D.; Pinnavaia, T. J. *Microporous Mesoporous Mater.* **1999**, *27*, 19.
(52) Marler, B.; Oberhagemann, U.; Vortmann, S.; Gies, H. *Microporous Mesoporous Mater*. **1996**, *6*, 375.
(53) Zhao, X. S.; Audsley, F.; Lu, G. Q. *J. Phys. Chem. B* **1998**, *102*, 4143.
(54) Adams, S.; Higgins, A. M.; Jones, R. A. L. *Langmuir* **2002**, *18*, 4854.
(55) Fu, F.-M.; DeOliveira, D. B.; Trumble, W. R.; Sarkar, H. K.; Singh, B. R. *Appl. Spectrosc*. **1994**, *48*, 1432.